



日本原子力研究開発機構機関リポジトリ
Japan Atomic Energy Agency Institutional Repository

Title	Organ absorbed dose estimation reflecting specific organ masses with simple scaling of reference doses using the organ masses
Author(s)	Manabe Kentaro, Koyama Shuji
Citation	Radiation Protection Dosimetry, 189(4), p.489-496
Text Version	Accepted Manuscript
URL	https://jopss.jaea.go.jp/search/servlet/search?5066982
DOI	https://doi.org/10.1093/rpd/ncaa058
Right	This is a pre-copyedited, author-produced version of an article accepted for publication in Radiation Protection Dosimetry following peer review. The version of record Organ absorbed dose estimation reflecting specific organ masses with simple scaling of reference doses using the organ masses is available online at: https://doi.org/10.1093/rpd/ncaa058 .

ORGAN ABSORBED DOSE ESTIMATION REFLECTING SPECIFIC ORGAN MASSES WITH SIMPLE SCALING OF REFERENCE DOSES USING THE ORGAN MASSES

Kentaro Manabe^{1,2,*} and Shuji Koyama³

¹Graduate School of Medicine, Nagoya University, Nagoya-shi, Aichi 461-8673, Japan

²Nuclear Science and Engineering Center, Japan Atomic Energy Agency, Tokai-mura, Ibaraki 319-1195, Japan

³Brain and Mind Research Center, Nagoya University, Nagoya-shi, Aichi 461-8673, Japan

Received month date year, amended month date year, accepted month date year

Estimating organ absorbed doses in consideration of person-specific parameters is important for optimisation of exposure doses by diagnostic nuclear medicine. This study proposes a straightforward method for estimating the organ dose that reflects a specific organ mass by scaling the reference organ dose using the inverse ratio of the specific organ mass to the reference organ mass. For the administration of radiopharmaceuticals labelled by ^{99m}Tc or ¹²³I, the organ doses for the liver, spleen, red marrow, and thyroid obtained by the method were compared with those generated by a Monte Carlo simulation. The discrepancies were less than 14% for the liver, spleen, and thyroid. Conversely, in some cases, the red marrow discrepancies were greater than 30% due to the wide distribution of red marrow in the trunk and head regions. This study confirms that the method of scaling organ doses can be effective for estimating mass-specific doses for solid organs.

INTRODUCTION

When radiopharmaceuticals are administered into the body, organs and tissues are exposed to the radiations emitted by the radionuclides within the body. In diagnostic nuclear medicine imaging, the precise estimation of organ absorbed doses (organ doses) is important for optimising the amount of radiopharmaceutical administration.

An absorbed dose D_T (Gy) of an organ or tissue T is obtained by⁽¹⁾

$$D_T = c_1 \sum_S \tilde{A}_S \sum_i E_i Y_i \text{SAF}(T \leftarrow S)_i \quad (1)$$

where c_1 (J MeV⁻¹) is a constant (1.602×10^{-13}) used to convert the unit from MeV to J, \tilde{A}_S (Bq s) is the number of disintegrations occurring in the source region S, E_i (MeV) and Y_i are the energy and yield of the i th radiation of the incorporated radionuclide, respectively, and $\text{SAF}(T \leftarrow S)_i$ (kg⁻¹) is the specific absorbed fraction (SAF), which is the fraction of the deposited energy per unit mass of T of the i th radiation to the T emitted from the S. The values of E_i , Y_i , and $\text{SAF}(T \leftarrow S)$ are obtained from literature^(2, 3), while the values of \tilde{A}_S are calculated based on biokinetic models⁽⁴⁾. However, the procedure used to estimate the D_T from basic dosimetric data using Equation (1) is quite complicated. The International Commission on Radiological Protection (ICRP) provides dose coefficients (the D_T per unit intake of activity) for the

administration of frequently used radiopharmaceuticals in units of mGy MBq⁻¹⁽⁴⁾. Therefore, organ doses can be easily estimated by multiplying dose coefficients by the amount of administration. Importantly, the organ doses obtained by this procedure are based on the physical characteristics of the reference person, which the ICRP has defined⁽⁵⁾. Considering individual physical characteristics, such as body weight and organ mass, is necessary to estimate a dose precisely, because organ doses are dependent on organ masses.

The most precise dose estimation can be achieved by performing a radiation transport calculation using a specific computational phantom with the same physical characteristics as the individual in question. However, such calculations are impractical due to their requirement for significant inputs of time and effort. The Committee on Medical Internal Radiation Dose (MIRD) has employed a methodology to scale SAFs for self-irradiation (self-SAFs), in which T is equal to S using the mass of the target in kg⁽¹⁾. In this methodology, self-SAFs for specific masses (SAF_{spec}) (kg⁻¹) are obtained by scaling self-SAFs based on a reference phantom (SAF_{ref}) (kg⁻¹), as

$$\text{SAF}_{\text{spec}} = \text{SAF}_{\text{ref}} \left(\frac{M_{\text{spec}}}{M_{\text{ref}}} \right)^{c_2} \quad (2)$$

where M_{spec} (kg) is the specific organ mass, M_{ref} (kg) is the organ mass of the reference phantom, and c_2 is a constant. The value of c_2 is set to -1 for electrons and $-2/3$ for photons and considers the difference in penetration ability between electrons and photons. Conversely, no correction is made for SAFs in the case of crossfire irradiation in which T is not equal to S

*Corresponding author: manabe.kentaro@jaea.go.jp

because of the compensating effects, as follows. The fractions of energy deposited in T will increase or decrease with increment or decrement of organ masses, respectively, because the target size will also change commensurately with the organ mass. However, in contrast, the dose will decrease or increase as the organ mass increase or decrease, respectively, because of the definition of dose. The effectiveness of this methodology has been confirmed for some cases of incorporation of radionuclides^(6, 7). However, several steps are required to calculate the D_T using Equation (1). To be successful in using this methodology, the administrator must have technical knowledge of dosimetric procedures or a specific calculation code to obtain the D_T value for a given organ mass. On this basis, the direct scaling of reference organ doses for default conditions using a specific organ mass is proposed to obtain the D_T based on a specific organ mass.

MATERIALS AND METHODS

Direct scaling method

The expression of the direct scaling method (DSM) to estimate the D_T considering the M_{spec} is as follows:

$$D_T = D_{\text{ref}} \left(\frac{M_{\text{spec}}}{M_{\text{ref}}} \right)^{-1} \quad (3)$$

where D_{ref} is the D_T based on a default phantom. Hereafter, the D_T values estimated by the DSM are referred to as D_{DSM} .

The values of the D_{DSM} along with those of the D_T obtained by a detailed calculation, D_{dil} , were compared to confirm the effectiveness of the DSM. The D_{dil} values were calculated based on self-SAFs evaluated by a Monte Carlo radiation transport calculation. A comparison was made for the intravenous administration of $^{99\text{m}}\text{Tc}$ -labelled colloids and for the oral administration of ^{123}I -labelled sodium iodine into adult males⁽⁴⁾. The former was selected due to the simple pharmacokinetics of $^{99\text{m}}\text{Tc}$ -labelled colloids and the high accumulation fractions for the liver, spleen, and red marrow. The latter shows high accumulation in the thyroid, whose shape is more complicated than that of either the liver or the spleen.

Pharmacokinetic data

Administered $^{99\text{m}}\text{Tc}$ distributes quickly to the liver, the spleen, and the red marrow in proportions of 0.7, 0.1, and 0.1, respectively, according to the pharmacokinetic data of $^{99\text{m}}\text{Tc}$ -labelled colloids⁽⁴⁾. The remainder of the $^{99\text{m}}\text{Tc}$ is assumed to uniformly distribute throughout the entire body other than the liver, the spleen, and the red marrow⁽⁴⁾. After the initial distribution of $^{99\text{m}}\text{Tc}$, neither the redistribution nor the excretion of $^{99\text{m}}\text{Tc}$ are

assumed to occur due to the relatively short physical half-life of $^{99\text{m}}\text{Tc}$ (6.05 h)⁽⁴⁾. In this study, the biological half-life in the blood was set to 1 min (equivalent to 1000 d⁻¹ as the transfer coefficient), which is a value often used by the ICRP in cases involving the immediate transformation of radioactivity^(8, 9). The transfer coefficient was split into four values based on the distribution proportions. The paths and their transfer coefficients (d⁻¹) are shown in Table 1. The same kinetics were assigned to ^{99}Tc , which is the progeny of $^{99\text{m}}\text{Tc}$.

It is well known that the thyroid is the target organ for administered iodine, and a number of models for the systemic kinetics of iodine have been published^(10–13). The latest one which is contained in ICRP Publication 137⁽⁹⁾ with the human alimentary tract model of ICRP Publication 100⁽¹⁴⁾ was applied to calculate the \dot{A}_S of the ^{123}I in the body. Table 2 lists the pathways and their transfer coefficients of the overall kinetic-model. The kinetics of $^{123\text{m}}\text{Te}$ and ^{123}Te , which are the radioactive progenies of ^{123}I , were assumed to be the same as that of ^{123}I presented in Table 2.

In both calculations, the amount of administered activity was set to 1 Bq. The initial activity for the administrations of $^{99\text{m}}\text{Tc}$ and ^{123}I was applied to the blood and the oral cavity, respectively.

Phantom scaling

This study used the Reference Computational Phantom for Adult Male (RCP-AM) developed by the ICRP⁽¹⁵⁾ as the reference phantom to calculate the self-SAFs for various masses. The RCP-AM is a volume-pixel (voxel) phantom. Thus, phantom scaling was performed by changing the voxel size of the tri-axial directions with the same scaling factors. The scaling factors were evenly distributed between 0.80–1.20 in increments of 0.05. The reason for this particular scaling range is discussed in the following paragraph.

The availability of statistical data related to organ mass distribution is quite limited. According to data from the Asian Reference Man⁽¹⁶⁾, a liver-mass distribution exhibits a normal-distribution. The arithmetic mean μ and the standard deviation σ of the liver masses of adult Japanese males are 1.62 and 0.36 kg, respectively. Therefore, the quotients of the 2.5th and 97.5th percentile values divided by μ are 0.561 and 1.439, respectively. When a phantom is scaled using the range between 0.8–1.2 as previously discussed, the mass variations range between 0.5–1.7. Thus, the chosen phantom-scaling range is sufficiently wide so that the effects of organ mass on D_T can be suitably determined.

Calculation of self-SAFs

A general-purpose Monte Carlo radiation transport code, MCNPX 2.6.0⁽¹⁷⁾, was utilised to calculate self-

SAFs incorporating the scaled RCP-AMs. The $e103^{(18)}$ and $mcplib04^{(19)}$ libraries were used as electron and photon cross-sectional data, respectively, and the cutoff energy was set at 1 keV for both electrons and photons. Secondary electrons produced by the interactions between primary photons and organs or tissues were also considered in the transport calculations. Computations were performed at 15 energy points ranging between 10–600 keV for both electrons and photons for the liver, the spleen, and the red marrow. For the thyroid, self-SAFs were evaluated up to 2 MeV at 19 points. The upper energy limits were determined from the maximum energy of the photons and electrons emitted from ^{99m}Tc and ^{123}I , according to the nuclear decay data published in ICRP Publication 107⁽²⁾. The number of histories was set to 10^5 for all calculations.

The ‘f6’ tally of the MCNPX, which obtains the deposited energy averaged over the designated region per unit mass E_{dpm} (MeV g^{-1})⁽¹⁷⁾, was used to determine the amount of energy deposited both on the liver and the spleen for both photon and electron transport. The ‘f6’ tally cannot be applied to the red marrow, because the red marrow is not segmented as a single tissue and is instead distributed in the spongiosa of the skeleton in the RCP-AM⁽¹⁵⁾. Therefore, E_{dpm} for the red marrow for photons was evaluated using dose-response functions (DRFs)⁽²⁰⁾ based on the following equation:

$$E_{\text{dpm}} = \frac{c_3}{M_{\text{rm}}} \sum_i M_i \int_0^{E_p} \Phi_i(E) \text{DRF}_i(E) dE \quad (4)$$

where c_3 (MeV J^{-1}) is a constant (6.242×10^{12}) used to convert the unit from J to MeV, M_{rm} (g) is the mass of the red marrow, M_i (kg) is the mass of the red marrow of the i th bone site, E_p (MeV) is the photon energy emitted from the red marrow, $\Phi_i(E)$ (m^{-2}) is the fluence in the i th bone site for the photon whose energy is E (MeV), and $\text{DRF}_i(E)$ (Gy m^2) is the energy-dependent DRF for the red marrow of the i th bone site. The fluence was obtained using an ‘f4’ tally implemented in the MCNPX⁽¹⁷⁾. The E_{dpm} in the red marrow for electrons was calculated by dividing the deposited energy in each bone site in accordance with the mass ratio of the red marrow to the bone site⁽²¹⁾. Finally, the self-SAFs were obtained using the following equation:

$$\text{SAF} = c_4 \frac{E_{\text{dpm}} M_{\text{nb}}}{E_{\text{rad}} M_{\text{wb}}} \quad (5)$$

where c_4 is a constant (10^3) used to convert from g^{-1} to kg^{-1} , E_{rad} (MeV) is the initial energy of the generated radiation, M_{nb} (kg) is the organ mass without blood, and M_{wb} (kg) is the organ mass with blood⁽³⁾. The ratio $M_{\text{nb}}/M_{\text{wb}}$ in Equation (5) was added to the SAF calculation procedure of the previous study⁽²²⁾ for consistency with the latest ICRP methodology⁽³⁾.

Calculation of D_{DSM} for other phantoms

The shapes of the bodies and the organs of both the original and scaled RCP-AMs are similar. The shapes of the evaluation objectives may affect the effectiveness of the DSM. Then, three phantoms were applied to verify the effectiveness of the DSM for people with different configurations to the original RCP-AM. One is the Reference Computational Phantom for Adult Female (RCP-AF), which has been developed as the reference phantom for adult females in the ICRP’s dosimetric methodology⁽¹⁵⁾. The others are the average adult Japanese male (JM-103) and female (JF-103) phantoms developed by Sato et al.^(23, 24). Their heights and weights are equal to the average values of adult Japanese males and females, and their organ masses are adjusted to the average values with relative errors between plus or minus 10%.

The D_{DSM} values of the organs of the RCP-AF, JM-103, and JF-103 were estimated using their organ masses as the M_{spec} , and the organ mass and the D_{T} of the RCP-AM as the M_{ref} and D_{ref} , respectively, in Equation (3). Then, the D_{DSM} results were compared with those of the D_{dil} based on the SAF datasets of the RCP-AF⁽³⁾, JM-103⁽²⁵⁾, and JF-103⁽²⁶⁾.

Calculation of D_{dil}

The internal dose calculation programme developed by Manabe et al.⁽²⁷⁾ was used to calculate the D_{dil} based on the default crossfire SAFs with the self-SAFs evaluated by Monte Carlo calculations. The Manabe’s programme utilises the latest dosimetric models and data provided by the ICRP to calculate effective and equivalent dose coefficients (Sv Bq^{-1}) in accordance with the ICRP 2007 Recommendations^(2, 3, 8, 9, 28, 29). The main feature of this programme is that the dosimetric models and data can be edited because the models and data files implemented in the programme are separated from the execution file and are recorded in a plain text format⁽²⁷⁾. For the administration of ^{99m}Tc and ^{123}I , the values of the equivalent dose coefficients (Sv Bq^{-1}) generated by the programme are equal to the absorbed dose coefficients per unit intake of activity (Gy Bq^{-1}). This is because the radiation weighting factors for photons and electrons are both one⁽²⁸⁾. After the calculation, the unit was manually converted from Sv Bq^{-1} to mGy MBq^{-1} .

Biokinetic data files for ^{99m}Tc -labelled colloids and ^{123}I -labelled sodium iodine were applied to the programme. Consequently, the photon and electron self-SAFs for the liver, the spleen, the red marrow, and the thyroid with those scaled by the eight kinds of factors described in the fourth section of this chapter were added. Furthermore, the SAF dataset for the RCP-AF of ICRP Publication 133⁽³⁾ and those for both JM-103 and JF-103 evaluated by Manabe et al.^(25, 26) were also implemented to the programme.

RESULTS

For all organs and energy points, the relative standard deviations of the calculated self-SAFs were smaller than 2%.

The numbers of disintegrations of ^{99m}Tc in the blood, the liver, the spleen, the red marrow, and the other tissues were 8.62×10^1 , 2.18×10^4 , 3.12×10^3 , 3.12×10^3 , and 3.12×10^3 , respectively. Table 3 lists the numbers of disintegrations in each organ for the oral administration of ^{123}I -labelled sodium iodine. The number of disintegrations of progenies of ^{99m}Tc and ^{123}I were, at most, approximately ten-thousandth of those of the parent nuclides. Therefore, the progenies' contribution to doses was negligible.

Figure 1 compares the values of the D_{dtl} and the D_{DSM} curve as a function of M_{spec} for the liver, the spleen, the red marrow, and the thyroid. When $M_{\text{spec}}/M_{\text{ref}}$ was less than one, the D_{DSM} was greater than the D_{dtl} in all organs. Conversely, when $M_{\text{spec}}/M_{\text{ref}}$ was more than one, the D_{DSM} was smaller than the D_{dtl} . Table 4 lists the values of D_{DSM} and D_{dtl} , and the discrepancies between the D_{DSM} and D_{dtl} for each phantom. The organ masses are also listed for reference.

DISCUSSION

Cause of the discrepancy between D_{DSM} and D_{dtl}

When a difference in organ mass exists (i.e. the size of the organ changes), there are changes not only in the mass, which is the denominator of the definition of the D_{T} , but also in the energy deposited in the organ, which is the numerator of the definition of the D_{T} ; these changes are due to the difference in absorbed fractions for self-irradiation (self-AFs). Figure 2 presents the correlation between $M_{\text{spec}}/M_{\text{ref}}$ and the self-AF of the liver for 141 keV photons which is the dominant radiation emitted from ^{99m}Tc due to nuclear decay, and 436 keV electrons of which energy is the maximum energy of beta particles emitted from ^{99m}Tc ⁽²⁾. The mass dependence of self-AFs for photons is higher than for electrons because of the high penetration ability of photons. In the MIRD methodology⁽¹⁾, the difference in the mass dependence of self-AFs between photons and electrons is considered by switching the constant c_2 in Equation (2). In contrast with the MIRD methodology, the DSM does not consider the size dependence of self-AFs for simplicity. Therefore, the DSM overcorrects the D_{T} values when the contribution of photons to the D_{T} is significant. For the intravenous administration of ^{99m}Tc -labelled colloids, the contribution proportions of photons and electrons to energy deposited in the liver by self-irradiation were 0.58 and 0.42, respectively, for the default organ mass. When $M_{\text{spec}}/M_{\text{ref}}$ decreased from 1.0 to approximately 0.5 (i.e. the scaling factor was 0.8), the photon self-AF decreased by 22%. Therefore, the DSM is expected to overcorrect the D_{T}

by approximately 13% by considering the proportion of the emitted energy as photons⁽²⁾. Crossfire irradiation also contributes to the liver dose. However, the discrepancy between the D_{DSM} and D_{dtl} can be explained only by the differences in self-irradiations, because the contribution due to crossfire irradiations was only 2% for the liver in the reference mass. The cause of the discrepancy for the spleen and the thyroid was the same as that for the liver.

The discrepancy between the D_{DSM} and D_{dtl} for the red marrow was larger than those for the liver, the spleen, and the thyroid. This result was because the DSM corrects the whole of the D_{T} without distinguishing between self- and crossfire irradiations. In this study, the crossfire irradiations accounted for 51% of the energy deposited in the red marrow. This percentage is much higher than that for the liver (2%). This high percentage was caused by the distribution characteristics of the red marrow in the body. The red marrow is widely distributed in the body⁽¹⁵⁾, and the radiation emitted from the red marrow can easily escape the source region.

These findings reveal that the result generated by the DSM depends on the portion of deposited energy derived from photons as well as the organ's distribution characteristics.

Effectiveness of the DSM

Organ mass has a significant effect on organ dose, especially when radioactivity accumulates in an organ. When the scaling factor was 0.8, the D_{dtl} value for the liver was 71% greater than the D_{ref} value; however, the discrepancy between the D_{DSM} and D_{dtl} was much smaller at only 14%. Similarly, the discrepancies between the D_{dtl} for each scaled RCP-AM and the D_{ref} were smaller than the discrepancies between the D_{DSM} and D_{dtl} in the spleen and the thyroid. The same tendency was observed in the phantoms containing different physical characteristics to those of the RCP-AM. Thus, the DSM is a simple and effective method to estimate doses that reflect the specific organ masses.

However, there are some points to be noted. It is possible that the D_{T} is underestimated when the organ mass is much greater than the reference mass. The accuracy of the DSM-estimated value depends on the proportion of photons and electrons that contribute to the D_{T} . As the contribution to doses due to photons increases, so the accuracy decreases. Additionally, the discrepancy between D_{DSM} and D_{dtl} will depend on the portion of the contribution due to self-irradiation. The application of the DSM may be inappropriate when a target organ or tissue is widely distributed in the body.

CONCLUSIONS

This study attempted the direct scaling of organ doses under default conditions using organ masses to obtain

doses that reflected specific organ masses. The doses obtained by the DSM were compared with doses evaluated using a radiation transfer Monte Carlo simulation. Consequently, the discrepancy between the direct scaled doses and the values determined by the detailed simulation was sufficiently small in terms of solid organs. The discrepancy between the doses by the DSM and the detailed simulation was increased by some factors, including the proportion of deposited energy due to photons to that of electrons and the particular distribution of organs or tissues in the body. In conclusion, the doses obtained by the DSM can be used for the purpose of optimising the administration of radiopharmaceutical for solid organs.

REFERENCES

- Snyder, W.S., Ford, M.R., Warner, G.G. and Watson, S.B. *MIRD Pamphlet No. 11: S, absorbed dose per unit cumulated activity for selected radionuclides and organs*. Society of Nuclear Medicine, New York (1975).
- International Commission on Radiological Protection. *Nuclear decay data for dosimetric calculations*. ICRP Publication 107. Ann. ICRP **38**(3) (2008).
- International Commission on Radiological Protection. *The ICRP computational framework for internal dose assessment for reference adults: specific absorbed fractions*. ICRP Publication 133. Ann. ICRP **45**(2) (2016).
- International Commission on Radiological Protection. *Radiation dose to patients from radiopharmaceuticals: a compendium of current information related to frequently used substances*. ICRP Publication 128. Ann. ICRP **44**(2S) (2015).
- International Commission on Radiological Protection. *Basic anatomical and physiological data for use in radiological protection reference values*. ICRP Publication 89. Ann. ICRP **32**(3–4) (2002).
- Petoussi-Henss, N., Bolch, W.E., Zankl, M., Sgouros, G. and Wessels, B. *Patient-specific scaling of reference S-values for cross-organ radionuclide S-values: What is appropriate?* Radiat. Prot. Dosim. **127**, 192–196 (2007).
- Wayson, M.B. and Bolch, W.E. *Individualized adjustments to reference phantom internal organ dosimetry—scaling factors given knowledge of patient internal anatomy*. Phys. Med. Biol. **63**, 085006 (2018).
- International Commission on Radiological Protection. *Occupational intakes of radionuclides: part 2*. ICRP Publication 134. Ann. ICRP **45**(3/4) (2016).
- International Commission on Radiological Protection. *Occupational intakes of radionuclides: part 3*. ICRP Publication 137. Ann. ICRP **46**(3/4) (2017).
- Riggs, D.S. *Quantitative aspects of iodine metabolism*. Pharmacol. Rev. **4**, 284–370 (1952).
- Committee on Medical Internal Radiation Dose. *Summary of current radiation dose estimates to humans from ^{123}I , ^{124}I , ^{125}I , ^{126}I , ^{130}I , ^{131}I , and ^{132}I as sodium iodine*. J. Nucl. Med. **16**, 857–860 (1975).
- International Commission on Radiological Protection. *Radiation dose to patients from radiopharmaceuticals*. ICRP Publication 53. Ann. ICRP **18**(1–4) (1988).
- Leggett, R.W. *A physiological systems model for iodine for use in radiation protection*. Radiat. Res. **174**, 496–516 (2010).
- International Commission on Radiological Protection. *Human alimentary tract model for radiological protection*. ICRP Publication 100. Ann. ICRP **36** (1–2) (2006).
- International Commission on Radiological Protection. *Adult reference computational phantoms*. ICRP Publication 110. Ann. ICRP **39**(2) (2009).
- Tanaka, G. and Kawamura, H. *Anatomical and physiological characteristics for Asian reference man. Male and female of different ages: Tanaka model*. NIRS-M-115 (1996).
- Pelowitz, D.B. *MCNPX user's manual version 2.6.0*. LA-CP-07-1473 (2008).
- Adams, K.J. *Electron upgrade for MCNP4B*. LA-UR-00-3581 (2000).
- White, M.C. *Photoatomic data library MCPLIB04: a new photoatomic library based on data from ENDF/B-VI release 8*. LA-UR-03-1019 (2002).
- International Commission on Radiological Protection. *Conversion coefficients for radiological protection quantities for external radiation exposures*. ICRP Publication 116. Ann. ICRP **40**(2–5) (2010).
- Snyder, W.S., Ford, M.R. and Warner, G.G. *MIRD pamphlet No. 5 revised: Estimates of specific absorbed fractions for photon sources uniformly distributed in various organs of a heterogeneous phantom*. Society of Nuclear Medicine, New York (1978).
- Manabe, K., Sato, K. and Endo, A. *Comparison of internal doses calculated using the specific absorbed fractions of the average adult Japanese male phantom with those of the reference computational phantom-adult male of ICRP publication 110*. Phys. Med. Biol. **59**, 1255–1270 (2014).
- Sato, K., Takahashi, F., Satoh, D. and Endo, A. *Construction of average adult Japanese voxel phantoms for dose assessment*. JAEA-Data/Code 2011-013 (2011).
- Sato, K. and Takahashi, F. *The contemporary JAEA Japanese voxel phantoms*. Radiat. Prot. Dosim. **149**, 43–48 (2012).
- Manabe, K., Sato, K. and Takahashi, F. *Assessment of specific absorbed fractions for photons and electrons using average adult Japanese male phantom*. JAEA-Data/Code 2014-017 (2014) (in Japanese).
- Manabe, K., Sato, K. and Takahashi, F. *Assessment of specific absorbed fractions for photons and electrons using average adult Japanese female phantom*. JAEA-Data/Code 2016-013 (2016) (in Japanese).
- Manabe, K., Sato, K. and Takahashi, F. *Estimating internal dose coefficients of short-lived radionuclides in accordance with ICRP 2007 recommendations*. J. Nucl. Sci. Technol. **56**, 385–393 (2019).
- International Commission on Radiological Protection. *The 2007 Recommendations of the International Commission on Radiological Protection*. ICRP Publication 103. Ann. ICRP **37**(2–4) (2007).
- International Commission on Radiological Protection. *Occupational intakes of radionuclides: part 1*. ICRP Publication 130. Ann. ICRP **44**(2) (2015).

Table 1. Pathways and their transfer coefficients for the intravenous administration of ^{99m}Tc -labelled colloids.

From	To	Transfer coefficient (d^{-1})
Blood	Liver	700
Blood	Spleen	100
Blood	Red marrow	100
Blood	Other tissues	100

Table 2. Pathways and their transfer coefficients for the oral administration of ^{123}I -labelled sodium iodine.

From ^{1,2}	To ^{1,2}	Transfer coefficient (d^{-1})
Oral cavity	Oesophagus (fast)	6.480E+03
Oral cavity	Oesophagus (slow)	7.200E+02
Oesophagus (fast)	Stomach contents	1.234E+04
Oesophagus (slow)	Stomach contents	2.160E+03
Stomach contents	Small intestine contents	2.057E+01
Small intestine contents	Right colon contents	5.940E+02
Small intestine contents	Blood-i	6.000E+00
Right colon contents	Left colon contents	2.000E+00
Left colon contents	Sigmoid colon contents	2.000E+00
Sigmoid colon contents	Faeces	2.000E+00
Blood-i	Thyroid-i	7.260E+00
Blood-i	Urinary bladder contents	1.184E+01
Blood-i	Salivary glands	5.160E+00
Blood-i	Stomach wall	8.600E+00
Blood-i	Other-i (rapid)	6.000E+02
Blood-i	Kidneys-i	2.500E+01
Blood-i	Liver-i	1.500E+01
Salivary glands	Oral cavity	5.000E+01
Stomach wall	Stomach contents	5.000E+01
Thyroid-i	Thyroid-o	9.500E+01
Thyroid-i	Blood-i	3.600E+01
Thyroid-o	Blood-o	7.700E-03
Other-i (rapid)	Blood-i	3.300E+02
Other-i (rapid)	Other-i (slow)	3.500E+01
Other-i (slow)	Other-i (rapid)	5.600E+01
Kidneys-i	Blood-i	1.000E+02
Liver-i	Blood-i	1.000E+02
Blood-o	Other-o (rapid)	1.500E+01
Other-o (rapid)	Blood-o	2.100E+01
Other-o (rapid)	Other-o (slow)	1.200E+00
Other-o (slow)	Other-o (rapid)	6.200E-01
Other-o (slow)	Blood-i	1.400E-01
Blood-o	Kidneys-o	3.600E+00
Kidneys-o	Blood-o	2.100E+01
Kidneys-o	Blood-i	1.400E-01
Blood-o	Liver-o	2.100E+01
Liver-o	Blood-o	2.100E+01
Liver-o	Blood-i	1.400E-01
Liver-o	Right colon contents	8.000E-02
Urinary bladder contents	Urine	1.200E+01

¹The compartments labelled '-i' are for inorganic iodine.

²The compartments labelled '-o' are for organic iodine.

Table 3. Number of disintegrations of ^{123}I in each source region for the oral administration of ^{123}I -labelled sodium iodine.

Source region	Number of disintegrations
Oral cavity	1.44E+01
Oesophagus (fast)	6.30E+00
Oesophagus (slow)	1.19E+01
Stomach contents	6.04E+03
Stomach wall	5.67E+02
Small intestine contents	2.07E+02
Right colon contents	3.81E+02
Left colon contents	2.34E+02
Sigmoid colon contents	1.44E+02
Blood	3.41E+03
Kidneys	8.39E+02
Liver	5.25E+02
Salivary glands	3.40E+02
Thyroid	1.42E+04
Urinary bladder contents	3.02E+03
Other tissues	9.87E+03

Table 4. Comparison of the D_{DSM} and D_{dtt} and the discrepancies between the D_{DSM} and D_{dtt} for various phantoms.

(a) The liver for the intravenous administration of $^{99\text{m}}\text{Tc}$ -labelled colloids

Phantom	M_{spec} (kg)	D_{DSM} (mGy MBq $^{-1}$)	D_{dtt} (mGy MBq $^{-1}$)	Discrepancy (%)
RCP-AM	2.360 ²	—	5.85E-02 ²	—
RCP-AM _{0.8} ¹	1.449	1.14E-01	9.96E-02	14
RCP-AM _{1.2} ¹	4.078	3.38E-02	3.84E-02	-12
RCP-AF	1.810	7.62E-02	7.25E-02	5.1
JM-103	1.462	9.44E-02	8.67E-02	8.9
JF-103	1.311	1.05E-01	9.37E-02	12

(b) The spleen for the intravenous administration of $^{99\text{m}}\text{Tc}$ -labelled colloids

Phantom	M_{spec} (kg)	D_{DSM} (mGy MBq $^{-1}$)	D_{dtt} (mGy MBq $^{-1}$)	Discrepancy (%)
RCP-AM	0.228 ²	—	6.07E-02 ²	—
RCP-AM _{0.8} ¹	0.117	1.18E-01	1.06E-01	11
RCP-AM _{1.2} ¹	0.394	3.51E-02	3.95E-02	-11
RCP-AF	0.187	7.40E-02	7.34E-02	0.82
JM-103	0.139	9.95E-02	9.58E-02	3.9
JF-103	0.110	1.26E-01	1.19E-01	5.9

(c) The red marrow for the intravenous administration of $^{99\text{m}}\text{Tc}$ -labelled colloids

Phantom	M_{spec} (kg)	D_{DSM} (mGy MBq $^{-1}$)	D_{dtt} (mGy MBq $^{-1}$)	Discrepancy (%)
RCP-AM	1.394 ²	—	8.03E-03 ²	—
RCP-AM _{0.8} ¹	0.714	1.57E-02	1.12E-02	40
RCP-AM _{1.2} ¹	2.409	4.65E-03	6.56E-03	-29
RCP-AF	1.064	1.05E-02	1.23E-02	-15
JM-103	1.192	9.39E-03	8.51E-03	10
JF-103	0.956	1.17E-02	1.08E-02	8.3

(d) The thyroid for the oral administration of ^{123}I -labelled sodium iodine

Phantom	M_{spec} (kg)	D_{DSM} (mGy MBq $^{-1}$)	D_{dtt} (mGy MBq $^{-1}$)	Discrepancy (%)
RCP-AM	0.0234 ²	—	3.58E+00 ²	—
RCP-AM _{0.8} ¹	0.0120	7.00E+00	6.66E+00	5.1
RCP-AM _{1.2} ¹	0.0404	2.07E+00	2.17E+00	-4.6
RCP-AF	0.0195	4.30E+00	4.31E+00	-0.23
JM-103	0.0202	4.15E+00	4.19E+00	-0.95
JF-103	0.0168	4.99E+00	5.01E+00	-0.40

¹The subscript number means the scaling factor.

²The organ mass and the D_{dtt} of the RCP-AM are the M_{ref} and D_{ref} values of Equation (3), respectively.

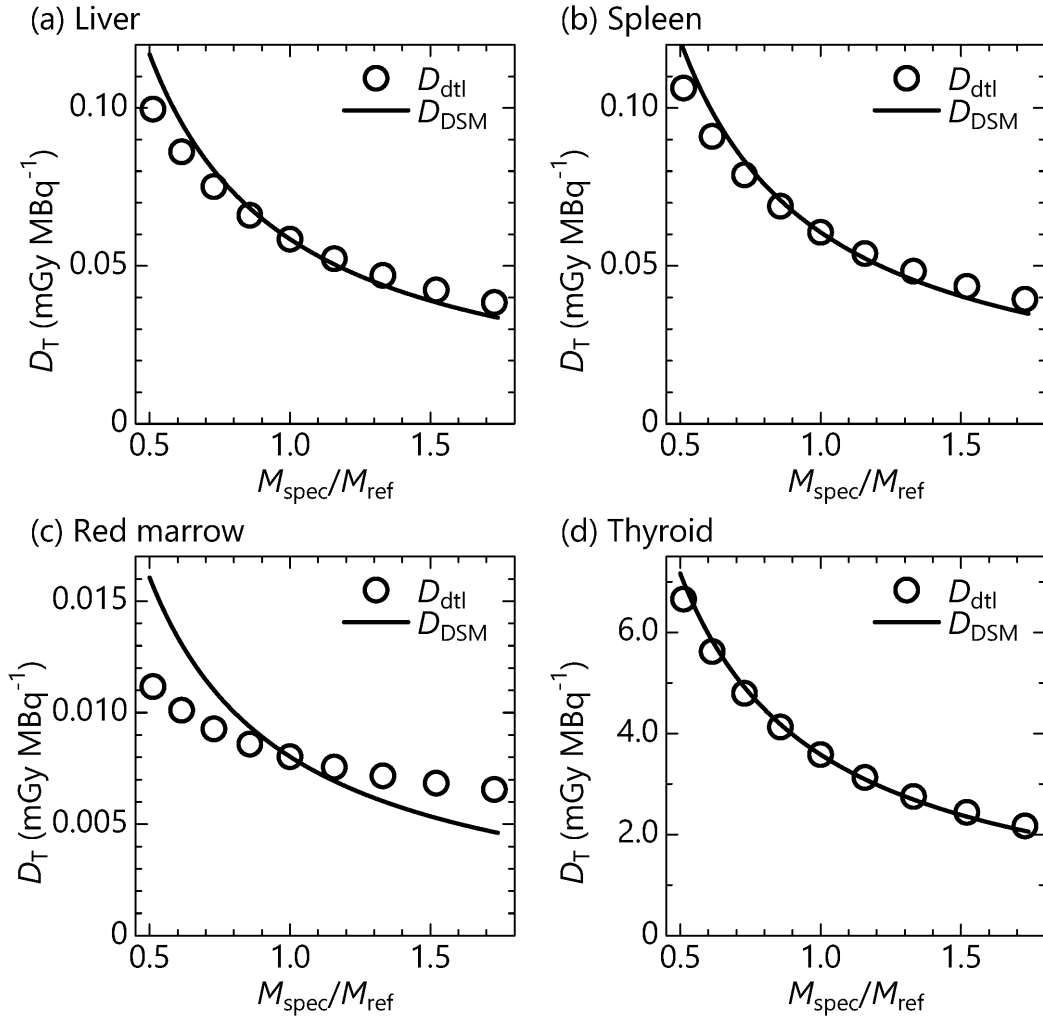


Figure 1. Correlation between $M_{\text{spec}}/M_{\text{ref}}$ and D_T for (a) the liver, (b) the spleen, and (c) the red marrow for intravenous administration of $^{99\text{m}}\text{Tc}$ -labelled colloids, and (d) the thyroid for oral administration of ^{123}I -labelled sodium iodine.

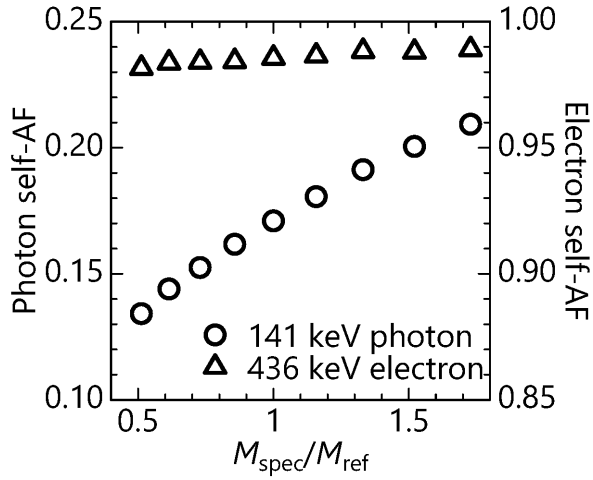


Figure 2. Self-AFs of the liver for 141 keV photons and 463 keV electrons. The left vertical axis indicates the self-AFs for photons, and the right one indicates those for electrons.